IJPSR (2013), Vol. 4, Issue 11 **(Research Article)**

INTERNATIONAL JOURNAL OF PHARMACEUTICAL SCIENCES AND RESEARCH

Received on 27 June, 2013; received in revised form, 28 July, 2013; accepted, 27 October, 2013; published 01 November, 2013

EXPRESSIONS PROFILING PROJECT OF HUMAN EMBRYONIC LUNG CELLSEXPOSED TO PYROLYZED CIGARETTE SMOKE

Klaus Braun*[1], Gabriele Müller [2], Matthias Schick [3], Melanie Bewerunge-Hudler [3], Oliver Heil [3], Manfred Wiessler [1], Rüdiger Pipkorn [4], Wolfhard Semmler [1] and Waldemar Waldeck [2]

German Cancer Research Center, Dept. of Imaging and Radiooncology [1], INF 280, D-69120 Heidelberg, Germany
German Cancer Research Center, Biophysics of Macromolecules [2], INF 580, D-69120 Heidelberg, Germany
German Cancer Research Center, Bioinformatics, Genomics & Proteomics Core Facility [3], INF 580, D-69120 Heidelberg, Germany
German Cancer Research Center, Central Peptide Synthesis Unit [4], INF 580, D-69120 Heidelberg, Germany

Keywords:

Cigarette smoke, Differential gene expression, Embryonic lung cells, Pyrolyzed smoke components

Correspondence to Author:

Dr. Klaus Braun

Medical Physics in Radiology, Deutsches Krebsforschungszentrum (DKFZ), Im Neuenheimer Feld 280, D-69120 Heidelberg, Germany

E-mail: k.braun@dkfz.de

ABSTRACT: In contrast to the problematic health and economic effects of acute and chronic smoke exposure on lung function and airway inflammation, there are still few data dealing with the effects of smoking. Smoke exposure can result in aberrant cell growth. In our experiments, pyrolyzed components of cigarettes have been shown to induce a strong stress response in cultured cells. We used human embryonic lung (HEL) cells, which respond with an altered expression of a broad spectrum of genes. Therefore we performed a systematic analysis of the genetic expression behaviour, using the established whole genome microarray-technology which should be able to reveal the cellular effects. With these data we aim to generate a qualitative spectrum of cellular stress response activity. It is noticeable that after cells' exposure to pyrolyzed tobacco smoke components the products of the most affected genes, e.g. *ID1, inhibitor of DNA binding*, are up-regulated as a rapid response after 2 h with a factor **3.8** and *RPS2, ribosomal protein S2*, is down-regulated to nearly 50 % after 24 hours. In databases they are documented as still uncharacterized and hypothetical proteins. The *DDIT4* gene, encoding the DNA-damage-inducible transcript 4, associated with regulation and development of DNA processes after damage by ionizing radiation and in p53 mediated apoptotic processes, is up-regulated. The exposure leads to a rapid cellular stress response of genes like induction of the *ID1*, *ID2*, and *ID3* genes, located on different chromosomes, already after two hours. They interact normally with DNA binding proteins under heterodimer formation and are considered as negative regulators of transcription. After 24 hours, a return back to normal was not observed and the genes remained stably down-regulated. The suppression of the *GADD45B* gene which is involved in the cell cycle regulation and after DNA damage a cell cycle arrest is mediated by the gene product. The *C14orf4* gene (*IRF2BPL*) suggests a bifunctional role in transcription control as a promotor's activator as well as a repressor. Recent data indicate a prominent role of this gene transcript in the control of female reproductive function. On balance, the role of the predominant amount of affected genes is focused on cellular stress response and DNA metabolism.

INTRODUCTION: According to the WHO statistics 2011, world-wide 12 million people got cancer in one year and approximately 7 million patients fall victim to the cancer per anno, thereof 5.4 million alone by tobacco smoke [1]. Patients, their family members, scientists and clinicians are aware of the urgent needs for development of more effective and more compliant pharmaceuticals against this dreaded and often invincible disease.

QUICK RESPONSE CODE

DOI: 10.13040/IJPSR.0975-8232.4(11).4203-22

Article can be accessed online on: www.ijpsr.com

DOI link: http://dx.doi.org/10.13040/IJPSR.0975-8232.4(11).4203-22

Tobacco smoke is considered as a leading cause for cancer. Furthermore it is undisputed that cigarette smoke is harmful for our health. Beyond dispute is also the fact that cigarette smoke contains over four thousand different and in part highly toxic constituents, which can act as stressors and can affect organs and organ systems of higher animals and humans, whose cells are subject to a complex intercellular exchange of information [2].

Adequate reactions and responses of cells to external stimuli, known as stressors including physical, chemical and biochemical are critical for appropriate physiologic operation procedures. Despite the opinion that small changes in gene expression represent noise and are not relevant [3], we measured moderate changes in expression of key genes which might influence metabolic pathways and result in altered cell phenotypes.

Each stimulus, which provokes an answer in the organism, is understood as a stressor in its physiological context [4]. Whereas some of the stressors are necessary and constant, some are incriminating but transient. Their quality and functionality mainly depends on the intensity. The cells' localization and molecular abilities play a major role with respect to the stressor's effects, possibly on designated target cells [5].

To respond to external stressors each cell type possesses specific surface receptors triggering intracellular signal cascades. If the stressor exceeds the cell's tolerable extent, it leads in the first instance to an induction of the cellular gene expression for maintenance of the homeostasis of the affected systems. But if the cell is not successful to reconstruct its natural metabolism, the programmed cell death (apoptosis) is activated. Moreover, if the stressor's effect on the cell is high enough to result in a collapse of the cellular functions, it is considered as a cell toxic agent. In this case triggering the cell to apoptosis is not possible anymore; the cell dies by necrosis.

Until today, methods using classical diagnostic histology tools supplemented with immune-histochemical techniques lead to a diagnosis of genetic diseases and possibly render the choice of the therapy. The validation of the cellular response at the mRNA level is more complex and needs molecular strategies, able to detect minimal changes in the gene expression of affected cells. With the rapid progress in the development of the microarray technology a new highly specific and sensitive tool was established in research and as a diagnostic tool in the foreseeable future. Therefore this array technology can be considered as an appropriate candidate which can do both, detect and quantify the induced or/and suppressed genes after external stimuli like chemical stressors (here constituents of tobacco smoke).

Experimental Section:

Cell culture: Human embryonic lung cells (HEL) (DKFZ Dept. B040) were cultured and maintained in DMEM (Gibco-BRL, Germany) and 10% fetal calf serum (Gibco-BRL, Germany) at 37°C in a CO_2 atmosphere.

Gene characterization using NCBI genomic databases:

- Reference Sequence database (RefSeq Version 8, www.ncbi.nlm.nih.gov/RefSeq/)

The collection aims to provide a comprehensive, integrated, well-annotated set of sequences, including genomic DNA, transcripts etc. RefSeq provides references for genome annotations, gene identification and characterization, expression studies, and comparative analyses.

- GenBank Version 9.0 (www.ncbi.nlm.nih. gov/genbank/)

It is the NIH genetic sequence database, an annotated collection of all publicly available DNA sequences.

- The data shown in the tables are detailed in the supporting Information with the extension "a".

Tobacco smoke (TS) constituents collection: The TS was dissolved in acetonitrile by shaking until the smoke was taken up by the solution. The smoke derived from 100 cigarettes (extract 2.5g). The dissolved residues were concentrated by use of a rotary evaporator (400 mbar, 38 °C) and, after desiccation with N_2 (1.5 - 2 bar) until total removal of the acetonitrile. The probe was stored in a freezer at -24°C.

Extraction of cigarette filters: The extraction of 100 cigarette filters containing 4.1g volatile and semi-volatile organic contaminants was carried out by the Soxhlet extraction method using 200 ml acetone as described by Saiki in 1909 [6]. The extraction was continuously cooled for 6 cycles for 60 minutes each. The acetone dissolved residues were concentrated by use of a rotary evaporator (400 mbar, 38 °C) and, after desiccation with N_2 (1.5 - 2 bar) stored in a freezer at -24°C.

Application of tobacco smoke residues and the filter extracts on HEL cells & RNA Isolation: The pyrolyzed tobacco smoke was kept on the HEL cells for 2 h & 24 h in a final concentration of 10 µM in cell culture medium. As controls untreated HEL cells were used. HEL cells were cultured as described in the methods section above. The pyrolyzed smoke residues were dissolved in medium and applied to the HEL cells in a final concentration of 10 µM. The culture medium was removed after 2 h or after 24 h. Cells were washed with Hank´s balanced salt solution. Total RNA from the HEL cells was isolated using the Qiagen RNeasy Plus Kit (Qiagen Hilden, Germany) according to the manufacture's instruction as follows:

The cells were washed twice with Hank´s solution and extracted with 1ml of Qiagen extraction solution. The cells were scraped and transferred into micro centrifuge-tubes, then the cells were homogenized by squeezing though a needle 0.9 × 12 mm followed by centrifugation through a DNA-Eliminator column for 30 sec at 10.000 rpm in a micro centrifuge.

An equal volume of 70% ethanol was added to the eluate, mixed with a pipette and applied to the RNeasy spin column. This was eluted with 700 µl RW1-buffer by centrifugation for 15 sec at 10.000 rpm followed by addition of RPE-buffer 2 × 500 µl and centrifugation at 10.000 rpm for 15 sec.

Then, the column was centrifuged to dryness and eluted by centrifugation with water (2 × 30 µl) for 30 sec and 2 min respectively. RNA was resuspended/eluted in TE/water. The quality of total RNA was checked by gel analysis using the total RNA Nano Chip assay on an Agilent 2100 Bioanalyzer (Agilent Technologies GmbH, Berlin, Germany).

The samples with RNA index values greater than 7 were selected for expression profiling. RNA concentrations were determined using the NanoDrop spectrophotometer (NanoDrop Technologies, Wilmington, DE).

Probe Labeling and Illumina Sentrix BeadChip array Hybridization: Biotin-labeled cRNA samples for hybridization on Illumina Human HT12- BeadChip arrays (Chip ID: 7196798076 (illumina_humanht-12_v4_r2) (Illumina, Inc. San Diego, CA) were prepared according to Illumina's recommended sample labeling procedure based on the modified Eberwine protocol [7].

In brief, 500ng of total RNA was used for complementary DNA (cDNA) synthesis, followed by an amplification/ labeling step (*in vitro* transcription) to synthesize biotin-labeled cRNA according to the Illumina® Total Prep™ RNA Amplification Kit (Life Technologies). Biotin-16-UTP was purchased from Roche Applied Science, Penzberg, Germany.

The cRNA was column purified according to TotalPrep RNA Amplification Kit, and eluted in 60-80 µl of water. Quality of cRNA was controlled using the RNA Nano Chip Assay on an Agilent 2100 Bioanalyzer and spectrophotometrically quantified (NanoDrop).

Hybridization was performed at 58°C, in GEX-HCB buffer (Illumina Inc.) at a concentration of 100 ng cRNA/µl, in a wet chamber for 20 h. Spike-in controls for low, medium and highly abundant RNAs were added, as well as mismatch control and biotinylation control oligonucleotides. Microarrays were washed once in High Temp Wash buffer (Illumina Inc.) at 55°C and then twice in E1BC buffer (Illumina Inc.) at room temperature for 5 minutes (in between washed with ethanol at room temperature).

After blocking for 5 min in 4 ml of 1% (wt/vol) Blocker Casein in phosphate buffered saline Hammarsten grade (Pierce Biotechnology, Inc., Rockford, IL), array signals were developed by a 10-min incubation in 2 ml of 1 µg/ml Cy3-streptavidin (Amersham Biosciences, Buckinghamshire, UK) solution and 1% blocking solution. After a final wash in E1BC, the arrays were dried and scanned.

Scanning and data analysis: Microarray scanning was done using an iScan array scanner. Data extraction was done for all beads individually, and outliers were removed when the absolute difference to the median is greater than 2.5 times the median absolute deviation (2.5 Hampel's method). All remaining bead level data points were than quantile normalized [8]. Amplified RNA syntheses from limited quantities of heterogeneous cDNA were performed using the free statistics software environment R.

As test for significance the student's t-test was used on the bead expression values of the two groups of interest. In the case of significance of expression against background we tested for greater than all negative beads for this sample and in the case of comparing separate groups we tested for inequality of the means of the groups. In both cases the Benjamini-Hochberg (HB) correction [9] was applied to the complete set of p-values of all 48107 ProbeIDs on the chip.

The average expression value is calculated as mean of the measured expressions of beads together with the standard deviation of the beads. We used an integrated genomics profiling and computational biology based strategy to identify the key genes and gene clusters whose expression was altered after exposure to pyrolyzed tobacco smoke residue.

Heatmap: The quantile normalized probe intensities have been used to calculate the heatmaps using R (heatmap.2 function). The cluster analysis, established by Eisen [10], describes the mean intensities of the affected genes according to their expression's pattern. Pearson correlation has been used to calculate the dendrograms of the heatmaps (corDist). Solely the probes were used with fold-change better than 2 and Benjamini-Hochberg corrected p-values smaller 0.001. To maintain clearness the fold-change cut off was adjusted to keep the number of displayed probes below 40

Principle Component Analysis - PCA Analysis: The PCA plot was done using Qlucore Omics Explorer 2.3 (Qlucore AB, Lund, Sweden) (http://www.qlucore.com/home.aspx). The quantile normalized mean intensities of all probes on the array in all analyzed samples were the bases. Log-transformation followed by a Multiple-Group-Comparison using the 5 different sample types allowed a filtering for probes better p-value 0.05. 4547 probes remained and were used to calculate the PCA-plot.

Network Generation: Our data sets containing the gene identifiers and corresponding expression values were uploaded to the Ingenuity application. Each gene identifier was mapped to its corresponding gene object in the Ingenuity Pathways Knowledge (IPA) Base (Ingenuity® Systems Inc., USA) [11]. A p-value, BH corrected cut off of <0.001 and fold change parameter with an expression value cut off >2 was set to identify genes whose expression was significantly and differentially regulated. These detected genes, called focus genes, were overlaid onto a global molecular network developed from information contained in the Ingenuity Pathways Knowledge Base.

Networks of these focus genes were then algorithmically generated based on their connectivity. The Core Analysis describes the assessment of signaling pathways. The data also give insight into networks and possible regulators upstream of the regulated genes.

Experimental design:

TABLE 1: T**HE LEFT COLUMN OF THE** Error! Reference source not found.**, CALLED "TABLE" LISTS THE NUMBERS (2-7) OF THE TABLES LISTING THE MAJOR AFFECTED GENES.** The right column relocates the detailed data of the group comparison measurements listed in the corresponding Tables (2a – 7a) in the supporting information.

Table	Group comparison	corresp. Table [Support. Inf.]
2	smoke_2h / smoke 24h	**2a**
3	filter_2h / filter 24h	**3a**
4	smoke_2h / control 2h	**4a**
5	smoke_24h / control 24h	**5a**
6	filter 2h / control 2h	**6a**
7	filter 24h / control 24h	**7a**

Dendrogram of the normalized data: A dendrogram visualizes the 'Pearson' distance between the measured samples and reflects the experimental setting of the replicates.

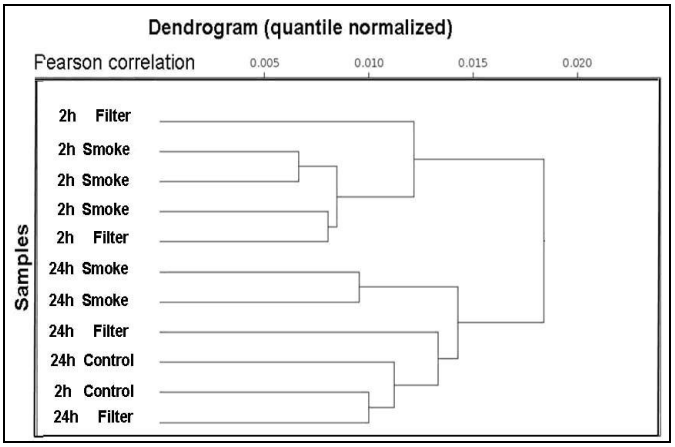

FIGURE 1: ILLUSTRATES THE DENDROGRAM OF THE CLUSTER-PRESENTATION OF THE NORMALIZED DATA OF THE DIFFERENTIAL GENE EXPRESSION PROFILING. The Pearson correlation coefficient reflects the degree of the correlation the two measured probes (**Error! Reference source not found.**).

Illumina chip expression analysis: Quality controls (QC), hybridization controls and negative controls of our samples are listed in the supporting information (**Figures 9a – 14a**). We started with the chip layout as shown in **Figure 2**.

Chip & Heatmap layout: With our data we designed a heat map, on the results listed above:

The differentiation between smoke and filter extracts makes sense as shown in the following coloured graph. The data of the ratios 24h vs. 2h smoke and filter, 24h vs. 24h untreated, and 2h vs.24h untreated control show the modified gene expression.

The ordinate demonstrates that the expression of stress affected genes induced or suppressed is strongly reduced after 24h, revealing a stress situation for the cells at 2h.

This can be interpreted from the lanes on the right side.

The abscissa represents the ratios between probes (smoke and filter) and untreated controls at the different time points.

Chip ID	Sample	Measurements after [h]	Extract
7196798076	Probe 1	2	Smoke
	Probe 4	2	Filter
	Probe 1	24	Smoke
	Probe 4	24	Filter
	Control	24	Control
	Control	2	

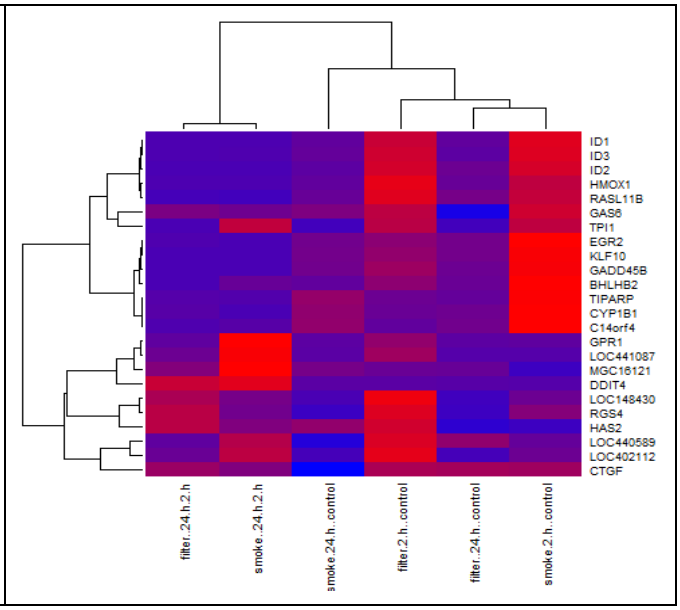

FIGURE 2: THE LEFT PART OF THE PICTURE PRESENTS OUR CHIP LAYOUT WITH PROBE1 REPRESENTING THE EXTRACTS OF THE SMOKE (2h/24h), PROBE4 (2h/24h) REPRESENTING THE FILTER, AND THE CONTROLS (2h/24h). The heat map (right part of the figure) illustrates the analysis of our Illumina Array data reflecting the differential gene expression in HEL cells measured as given in Table 3 - Table 7. The cluster analysis, established by Eisen [10], describes the genes according to their gene expression patterns (induced – red; suppressed – blue) with known function. The array also includes genes with still unknown function (Up-regulated genes are also displayed in red; down-regulated genes in blue (Down-regulated  up-regulated).

Principle Component Analysis (PCA): To define the correlation between our triplicate probes a PCA was carried out as described in the experimental section.

The plot (**Figure 3**) shows a perfect correlation between 3 probe replicates and a clear separation of the analyzed sample types.

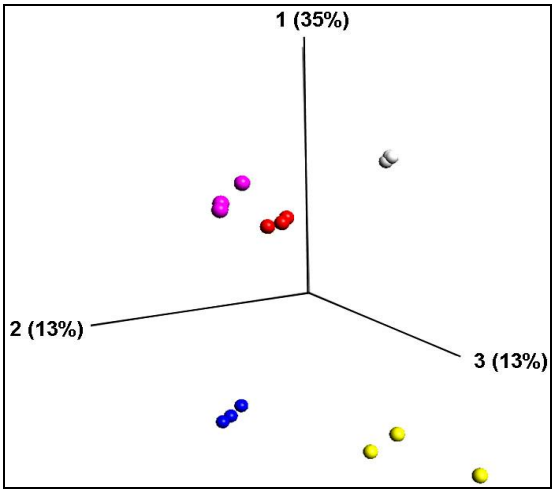

FIGURE 3: SHOWS THE PCA PLOT WHICH REPRESENTS THE QUALITY OF THE EXPERIMENT. The centerlines show the principal components 1-3. The sample types are: ■ smoke 2h; ■ smoke 24h; ■ filter 2h; filter 24h; □ control 2h/24h

Pathway analyses using Ingenuity Pathways Analysis (IPA) software Pathway analyses give insight into the complex regulation responses to smoke ingredients-based gene activation or inactivation. The datasets list and interpret the 606 affected genes (cut off: fold change >2 and p-value Benjamini-Hochberg (HB) corrected <0.001) except hypothetical genes.

The *Core Analysis* in this program generates a graphic presentation of molecular processes relevant to tobacco smoke ingredients exposition.

The *network analysis* illustrates graphically the top networks implement in the pathway analysis like in

1. Cell death and survival;
2. Cellular growth and;
3. The topics of bio function like diseases and disorders;
4. Molecular and cellular functions, as shown in the upper part of the corresponding **Tables 2 – 7**.

The major affected genes were subdivided into sections as shown in Table 1 and in Table 1a, supporting information), whose "biological functions" are described in the text according to the Gene Ontology (GO) terms. The corresponding scatterplots (shown in **Figures 3a – 8a**, supporting data) describe the expression differences (between the upper left dots and the lower right dots are shown in the supporting information.

Differential analyses: Detailed data can be found in supporting data (Gene loci, size of changes and p-values of groups against controls).

RESULTS AND DISCUSSION: Tobacco smoke extracts were collected as described in the experimental section. They were applied to human embryonic lung cell cultures (HEL). The cells then were investigated at two time points (after 2 hours and 24 hours). RNA was extracted, reversely transcribed and applied to microarrays. The cellular expression profile, affected with tobacco smoke components, was evaluated using R analysis as described in the scanning and data analysis section. We were able to identify a broad spectrum of differentially expressed genes.

Many genes appeared to be diversely involved, but in order to avoid a feared search for a needle in a haystack we selected the most prominently changed genes. For a better understanding, these mainly affected genes were subdivided first, according to their parameters to an early and late reaction as well as induced and suppressed genes (see database ArrayExpress accession E-MTAB-1378). In a second step, the altered state after treatment and the gene ontology annotations of the up- and down-regulated genes in HEL cells were listed. We built tables with R analysis with the Illumina Chip ID number (7196798076), gene loci, and GenBank Accession number according to the expression analysis instructions [12; 13].

Total RNA from HEL cells either untreated or cigarette smoke components exposed were characterized in technical triplicates. Based on the fact that the identified proteins can fulfil multifaceted and specific functions, we suggest that the characterization of the corresponding affected genes can be illustrated by division into the differential gene expression categories as summarized in Table 1 and in 1a, namely tobacco smoke/ main current: gene expression ratio after 2 h and 24 h, documented in Table 2 and in the supporting information, Table 2a, tobacco smoke/ cigarette filter: gene expression ratio after 2 h and 24 h, in Table 3 and in Table 3a, tobacco smoke/

main current/ untreated control cells: gene expression ratio after 2 h, in Table 4 and in table 4a, tobacco smoke/ main current/ untreated control cells: gene expression ratio after 24 h, in Table 5 and in Table 5a, tobacco smoke/ cigarette filter/ untreated control cells: gene expression ratio after 2 h, in Table 6 and in 6a , and tobacco smoke/ cigarette filter/ untreated control cells: gene expression ratio after 24 h, shown in Table 7 and in Table 7a.

Although the array data show an aberrant gene expression, the genes' functions, like the *MGC16121* (induced **3.4** fold, 2h after exposition), and the *C140rf4* (induced **3.34** fold, 2h after exposition) are still uncharacterized. A further finding is the strong suppression of genes with the exception of the *DDIT4* gene which is induced **7.88** fold at 24 h after exposition to components from main current tobacco smoke and also from cigarette filters **6.69** fold.

TABLE 2: AFFECTED GENES – EXPRESSION RATIO 24H & 2H AFTER EXPOSITION TO TOBACCO SMOKE COMPONENTS.

TABLE 3: AFFECTED GENES – EXPRESSION RATIO 24H & 2H AFTER EXPOSITION TO FILTER EXTRACTS

Pathway and Network Analysis

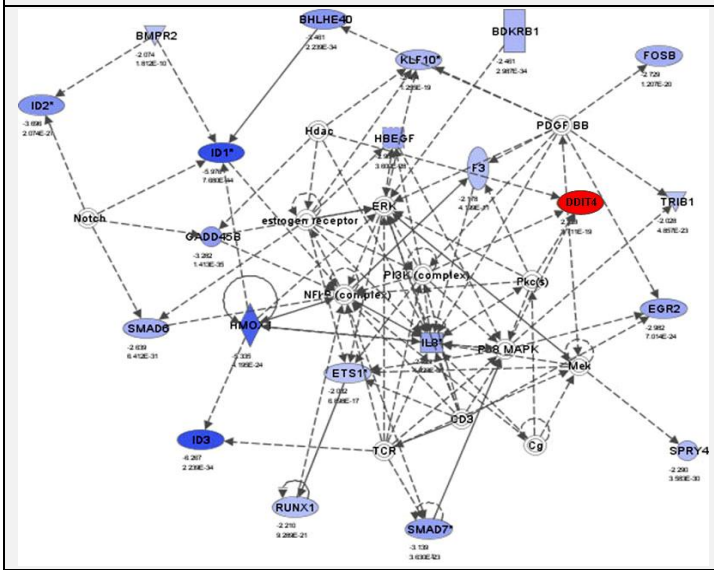

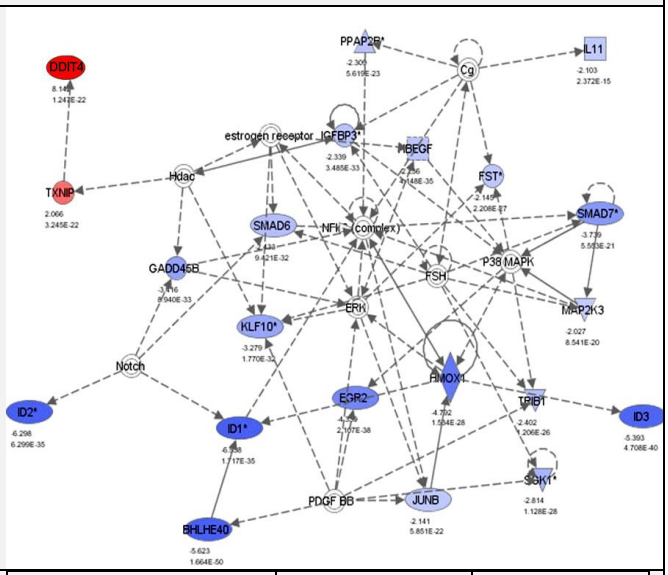

Gene Product (Gene)	RefSeq AC No.	Ratio smoke 24 h/2 h
DDIT4	NM_019058.2	**7.88**
MGC16121	NR_024607.1	**3.34**
ID1	NM_181353.1	**0.14**
ID2	NM_010496.3	**0.15**
ID3	NM_008321.2	**0.18**
HMOX1	NM_002133.2	**0.22**
EGR2	NM_000399.3	**0.26**
KLF10	NM_005655.2	**0.3**
GADD45B	NM_015675.3	**0.3**

Gene Product (Gene)	RefSeq AC No.	Ratio filter 24 h/2 h
DDIT4	NM_019058.2	**6.69**
ID3	NM_008321.2	**0.14**
ID1	NM_181353.1	**0.14**
ID2	NM_010496.3	**0.18**
HMOX1	NM_002133.2	**0.19**
KLF10	NM_005655.2	**0.3**
GADD45B	NM_015675.3	**0.3**

It becomes apparent in Table 2 that the cellular response against pyrolyzed tobacco is high. The ratio of the different gene expression at 2h and 24 h after exposition indicates a couple of induced genes (factors **7.88** and **3.34**) and genes which are clearly suppressed (between factor **0.15** and **0.3**).

These data show that the cigarette filter can retain only partially the mainstream tobacco smoke components [14-17] as emphasized also by the Harris and Novotny groups [18; 19]. However, protection effects for all cells of the respiratory system also after the resorption of agents toxic for sensible organs across the epithelial layer into the organism seem to be apparent [20].

The Table 3 lists the most affected genes by filter extracts. The analysis of the genes reflects a clear induction (**7.88**) of the *DDIT4* gene (NM_019058.2 – Homo sapiens DNA-damage-inducible transcript 4) encoding the DNA-damage-inducible transcript 4 gene product (accession no NM_005328.1). The gene maps at 10q22.1. The corresponding mRNA is mentioned in "Mammalian Gene Collection (MGC), offering data of status, quality and expansion of the NIH-full length cDNA project [21]. The search in the NCBI database "HomoloGene" (http://www.ncbi.nlm.nih.gov/homologene) of the *CDDIT4* gene finds a broad conservation from human to fish, (chimpanzee, dog, cow, mouse, rat, and zebrafish). The molecular protein's function is well documented in AmiGO Gene Ontology (http://amigo.geneontology.org/cgi-bin/amigo/term_details?term=GO:0071889). The protein interacts with the highly conserved "14-3-3 proteins" whose dimers are critically implicated in the modulation of multiple biological processes [22].

Recent findings describe the DDIT4 as an interacting protein for the regulation of the mTOR activity under hypoxia [23]. DDIT4 also acts as mediator of signal transduction by the factor "Akt" (serine/threonine-specific kinase) in diabetic muscle atrophy [24].

An increased induction from 2 hours to 24 hours (**3.34**) of a gene encoding the still hypothetical protein mapped at Xq26.3 is documented as NR_024607.1 uncharacterized protein - MGC16121. It is conspicuous that this gene shows a distinctly measured stress response against components of the cigarette smoke, but it is still uncharacterized as shown in the NCBI database PubMed (search of July 20 2012) which finds one publication and documents an involvement of this gene product in the regulation of the *DNMT3A* gene under extremely low frequency magnetic fields studies (ELF-MF) on monocytes in which an increased ROS release was detected [25].

The mRNA encoding the MGC16121 hypothetical protein is involved in the ROS-induced cellular stress response and possibly to chemical components occurring in tobacco smoke. This allows first speculations of its biochemical role.

A gene suppression ratio (**0.14**; **0.15**; **0.18**) is revealed with NM_181353.1/ NM_010496.3/ NM_008321.2 at a similar level. These genes are documented as dominant negative helix-loop-helix proteins (ID1; ID2; ID3) human inhibitors of DNA binding, consisting of three transcription variant members. They map on three different chromosomes: **20q11**; **2p25**; **1p36.13-p36.12**. The proteins encoded by these genes are able to form heterodimers with gene products of the HLH family of transcription factors, and can therefore reduce or inhibit the binding capacity of the basic HLH proteins [26; 27].

The involvement of *ID1* in biological processes as a modulator of the frequency, rate or extent of angiogenesis is described as GO: 0045765. GO: 0000122 documents pivotal negative regulation of transcription of the RNA II polymerase promoters.

The link to: http://www.ebi.ac.uk/QuickGO/GTerm?id=GO:0000122#term=annotation emphasizes the key role of this gene and gives an overview in the spider's web like signal transduction network. The search for *ID2* in http://amigo.geneontology. org/cgi-bin/amigo/gp-assoc.cgi?gp=UniProtKB: Q02363&session_id=3182amigo1342678291 finds annotations in regulation of biological processes: GO:0048469 documents the role in the cellular development, morphogenetic change which is required for a cell to attain its fully functional state.

General annotations are documented for the *ID3* gene, whose gene product is expressed abundantly in lung, kidney and adrenal gland, as an inhibitor of transcription of E2A-containing protein complexes in the cell nucleus (GO:0005634) [28] (http://www.uniprot.org/uniprot/Q02535). Gene ontologies demonstrate roles in biological processes: in the development of the central nervous system (GO:0007417), in a change of activity of a cell or an organism (in terms of movement, secretion, enzyme production, gene expression, etc.) as a result of a stimulus indicating damage to the organism (GO:0009611).

The next suppressed gene is the *HMOX1* homo sapiens heme oxygenase (decycling) 1 gene (NM_002133.2). In the NCBI Database "PubMed" are 1006 articles (between 1989 and 2012) which accentuate the scientific relevance of this gene and its product. *HMOX1* is mapped at chromosome **22q13.1**. An induction of HMOX1 by multifaceted stressors, like cadmium [29], inflammatory stimuli [30], and oxidative stressors [31] is well documented and may protect cells under various stress conditions in the endothelium. The HMOX1 gene product is a membrane-bound enzyme (GO: 0043231), localized to microsomes (GO: 0005792) and the endoplasmic reticulum (GO: 0005783).

Here we could detect a transcriptional repression of *HMOX1* (**0.22**). A study published in 2012 by Garbin et al revealed a stress-induced suppression of the heme oxygenase-1 (*HO-1*) in endothelial dysfunction of young smokers [32].

Searches in AmiGO (http://amigo.geneontology. org), UniProt (http://www.uniprot.org /uni

prot/B1AHA8), and in the EMBL-EBI (http://www.ebi.ac.uk/QuickGO/GProtein?ac= B1AHA8) found a key role of HMOX1 in the DNA damage response and signal transduction resulting in induction of apoptosis (GO: 0008630).

A deficiency of the *HMOX1* correlates with complex disorders such as iron metabolism [33;34], and a loss of protection against ROS generating vascular NADPH oxidase [35].

Another suppressed (**0.3**) gene is the homo sapiens Krüppel-like factor 10 (NM_005655.2). *KLF10* mapped at **8q22.2**. In the EMBL-EBI database (http://www.ebi.ac.uk/QuickGO/GProtein?-ac=Q13118) a lot of GO annotations is listed. The database UniProt (http://www.uniprot.org/ uniprot/Q13118) describes the KLF10 product as transforming growth factor-β-inducible early growth response protein 1. GOs of "biological processes" indicate a transforming growth factor β receptor signaling pathway [36]. GO: 0005634 documents KLF10 as "cellular component" in the nucleus; GO:0003677 and GO:0008270 highlights its "molecular functions" as a gene product which interacts selectively with DNA and non-covalently with zinc ions [37;38]. Data suggest that KLF10 may act as a tumor suppressor [39; 40]. KLF10-mediated transactivator studies detect a novel von Hippel-Lindau (VHL) target gene, which is associated with vascular kidney, brain and adrenal gland tumors. The role of *KLF10* under hypoxic conditions, also provoked by components of tobacco smoke, may affect the tumorigenesis. This implication, however, remains to be elucidated [41].

A clear suppression of the EGR2, the homo sapiens early growth response factor 2 (NM_000399.3) expression ratio was measured after 2 h and 24 h of (**0.26**). Aberrant expression rates or loss of function in this case can result in neuropathological diseases as recently documented in genetic and molecular diagnosis studies [42;43]. They are associated with Charcot-Marie-Tooth disease [44]. EGR2 is mapped at **10q21.1** and encodes three tandem C2H2-type zinc finger motifs harboring transcription factor E3 functional as SUMO-protein ligase. EGR2 has a binding affinity to the HOXA4 promotor (http://www.uniprot.org/uniprot/P11161). GO:0005634 lists EGR2 as a nuclear component bound inside of the nuclear envelope. The broad conservation from humans down to aspergillus flavus points to its functional importance for the formation and maintenance of the neuroprotective myelin responsible for transmission of nerve impulses [45;46].

We also detected a GADD45B's suppression with the coefficient of **0.3**. It is a homo sapiens growth arrest and DNA-damage-inducible, β gene mapped at chromosome **19p13.3**. The search in PubMed (2012, July 20) finds a first publication on the association of the gene product MyD118 with apoptosis of myeloid leukemia cells by the Hoffman group in 1994 [47].

In the UniProt database the protein's denotation "negative growth regulatory protein MyD118" derived from these studies [48], whereas nowadays the term "Growth arrest and DNA damage-inducible protein GADD45 β protein" is preferred (http://www. uniprot.org/uniprot/O75293 and [49]), GO:0030154 in the category "biological process". The protein is involved in apoptosis which begins when cells receive internal (e.g. DNA damage) or external death signals (GO: 0006915 and [50-53]). The GO category "molecular function" describes the product as a developmental protein involved in the

development control of multicellular organisms from its early immature forms to an adult (GO:0007275) [54-56]). Recent molecular profiling studies suggest the GADD45's pivotal role in tumorigenesis, under hypoxic conditions, as documented in von Hippel-Lindau patients' studies [57]. The repression of the tumor suppressor gene GADD45B in endothelial cells is important for anti-tumor responses [58-61] and seems to be correlated to a loss of function after exposition to tobacco smoke components.

Our data confirm the results of a study published in 2008 by Thompson and Burcham [62] regarding the above mentioned genes. Our group likes to join the colleagues' perception, that future work is needed to detect not only genes like *EGR2*, *HMOX1*, and *GADD45B*, which are acrolein-responsive and contribute to cell and tissue injury in the smoke-exposed lung.

Therefore it is important to note that acrolein, as a tobacco smoke component, impacts the gene expression of different gene groups in our study. It is widely accepted that acrolein participates in many diseases, including lung cancer.

The graphs illustrate the IPA phenotypic view of the network of gene expression response induced by tobacco smoke. The main affected genes influenced by tobacco smoke are highlighted in blue and red circles. The association of the genes found, generated a network map with the known connections of the affected genes which indicates differential gene expression mechanisms.

The IPA analysis settings show the top networks. Network 1 (Table 2) with 16 scores describes the network functions cell death and survival, cellular growth and proliferation. *EGR* is associated in the network 3 which represents the functions cancer, endocrine system. *GADD45B* and *MGC16121* are involved in the network 5 which comprehends the functions cell cycle and endocrine system disorders, except the *MGC1612*, which is still uncharacterized.

The following section highlights the cellular stress response of HEL cells against the smoke constituents extracts measured under identical conditions.

TABLE 4: AFFECTED GENES – EXPRESSION RATIO 2H CONTROL & 2H AFTER EXPOSITION TO TOBACCO SMOKE COMPONENTS

TABLE 5: AFFECTED GENES – EXPRESSION RATIO 24H CONTROL & 24H AFTER EXPOSITION TO TOBACCO SMOKE

Pathway and Network Analysis

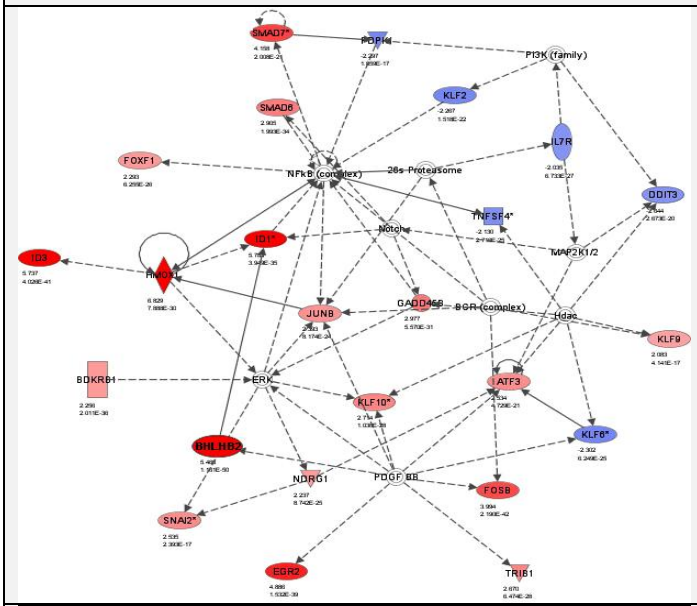

No pathway / network available

Gene Product (Gene)	RefSeq AC No.	Ratio smoke 2 h/ control

Gene Product (Gene)	RefSeq AC No.	Ratio smoke 24 h/ control

ID3	NM_008321.2	**5.54**
CYP1B1	NM_000104.3	**4.57**
ID1	NM_181353.1	**5.78**
ID2	NM_010496.3	**5.73**
HMOX1	NM_002133.2	**6.33**
TIPARP	NM_015508.4	**5.23**
BHLHB2	NM_003670.2	**5.73**
RASL11B	NM_023940.2	**3.69**
C14orf4	NM_024496.2	**3.34**
CTGF	NM_005328.1	**0.25**
TPI1	NM_000365.5	**0.35**
GPR1	NM_005279.3	**0.44**
Predicted ***LOC148430***	XR_038750.1	**0.46**
Similar to ***RPS2 variant 3***	NG_010039	**0.47**
RPS2	NM_002952.3	**0.48**
Predicted ***LOC402112***	XR_019262.2	**0.48**

The Table 4 lists the most affected genes with a rapid response at 2 hours after exposition to tobacco smoke components compared to the gene expression profile of untreated HEL cells as a control. It is evident that all coefficients reveal an induced gene expression as cellular stress response after 2 hours (as listed in Table 2 and Table 3). Furthermore the following genes feature a rapid induction of the gene expression.

The genes listed on Table 4 show an increased induction after already 2 hours (**4.57**) of NM_000104.3, documented as homo sapiens cytochrome P450, family 1, subfamily B, polypeptide 1 gene (CYP1B1). It is mapped at **2p22.2** and encodes a monooxygenase enzyme critical in drug metabolism and cholesterol biosynthesis (http://www.genecards.org/cgi-bin/carddisp.pl? gene=CYP1B1& search=CYP1b1) (GO: 0004497). It has an apparently important function as accounted by the scores of publication data of 1520 in PubMed (search from 2012 July 20). The cytochrome P450 1B1 was characterized by Ingelman-Sundberg [63]. The critical associations of the gene-isoforms in neoplastic processes were already obvious in estrogen metabolism studies (GO: 0008210) [64-66].

The data of the PRJNA study (Effects of tobacco smoke on gene expression and cellular pathways in a cellular model of oral leukoplakia published by the Weinstein group in 2008) give insight into a causally association of tobacco smoke constituents to the formation of multiple tumor types and simultaneously a decreased anticancer treatment efficiency was observed. Cytochrome P450 1B1 interacts with the hydrocarbon receptor. Analysis of networks found aryl hydrocarbon receptor (AhR)-dependent genes, like the xenobiotic metabolizing enzyme CYP1B1 (GO: 0006805) increased in oral mucosa of smokers [67]. The data confirm a pivotal association of the AhR in the genetical stress response provoked by chemicals occurring also tobacco smoke [68-70].

We also found a rapid induction (**5.23**) of NM_015508.4. It is described as the homo sapiens 2, 3, 7, 8-tetrachlorodibenzo-p-dioxin (TCDD)-inducible poly(ADP-ribose) polymerase (TIPARP) gene. TIPARP is cytogenetically mapped at 3q25.31b and encodes the nuclear protein TIPARP (GO: 0003676) [71]. It acts as a poly[ADP-ribose]polymerase using NAD(+) (http://www. genecards.org/cgi-bin/carddisp.pl?gene=TIPARP &search= TIPARP).

The gene product plays a central role to chemicals like TCDD as shown in the study of patterns of dioxin-altered mRNA expression (PRJNA110117) [72]. The complete GO annotations are listed in the EMBL-EBI database (European Bioinformatics Institute) (http://www.ebi.ac.uk/QuickGO/GProtein?ac=C9JXM5). First published was TIPARP by the Dong group in 2001 [73].

We found an induced (**5.73**) *BHLHB2* gene. The RefSeq Number NM_003670.2 characterizes the gene of the homo sapiens basic helix-loop-helix domain, class B, 2. It is located at the cytogenetic band **3p26.2a** [74], expressed in various cells like chondrocytes documented by the Kato group in 1997 [75]. Ontology "biological process" describes an involvement of the nuclear BHLHB2 protein (GO: 0005634) in the negative regulation of genes harboring an E-box DNA motif (GO: 0070888) involved in gene modulation of the circadian rhythm in mammals in the hypothalamus [76; 77]. A further BHLHB2 protein's key role is the strong expression control in cellular differentiation processes. It is abundantly expressed in colon carcinomas, but not in the surrounding normal tissues [78]. However, the association with these data has not been thoroughly established and requires further investigations to understand hypoxia and metastatic behavior in melanoma cells [79].

We measured an induction (**3.69**) of the homo sapiens RAS-like, family 11, member B (*RASL11B*) gene NM_023940.2. This gene is a member of the GTPase protein family (GO: 0003924), associated in central oncogenic-deregulated tumorigeneic neoplasm processes and the high conservation in chimpanzee, dog, cow, mouse, rat, chicken and zebra fish (as shown in the NCBI database HomoloGene).

Currently, knowledege regarding this gene remains rather limited. PubMed search (2012 July 23) resulted in as few as six matches which document the mapping at the chromosomal segment **4q12a** [80], and characterize the genomic organization of *RASL11B* as well as the tissue-specific expression patterns. Exact function of RASL11B is still not fully understood. A Norwegian microarray-based xenograft study was carried out and published in 2012. The Myklebost group concluded that a gained aberrant gene expression could be the result of general tumor progression in xenografts [81].

We observed an induction (**3.34**) of the homo sapiens chromosome 14 open reading frame 4 (*C14orf4*) [82], an intronless human gene containing a polyglutamine repeat, first characterized by Danieli [83]. It is mapped to the arrhythmogenic right ventricular dysplasia 1 critical region (ARVD1) of **14q24.3a**. ARVD is a dominantly inherited disorder which is one of the major causes of juvenile sudden death [84]. The NCBI Reference Sequence (RefSeq) NM_024496.2 specifies the gene as "Homo sapiens interferon regulatory factor 2 binding protein-like" (IRF2BPL) whose gene product represents a nuclear phosphor protein (GO: 0005634) [85] and may contribute to the control of female reproductive function [86]. In the http://www.uniprot.org/uniprot /Q9H1B7#section database it is documented in the GO sections "biological process" (GO: 0008150), "molecular function" (GO: 0003674).

The IPA analysis detected the following top networks. The graphical presentation of the network 1 with the highest score is shown in Table 4 and illustrates genes and the associated network functions, cell death and survival, cell-mediated immune response, and cellular function. Further detected top networks describe cell to cell signaling and interaction, cellular movement (network 2), cancer, cellular development (network 3), cellular growth and proliferation, gene expression (network 4), and cancer, organ development respiratory disease (network 5).

The Table 5 lists the most affected genes 24 hours after exposition to tobacco smoke components compared to untreated HEL cells as a control. It is conspicuous that all coefficients reveal a suppressed expression as cellular late stress response. The IPA analysis of Table 5 detected the following networks. The network 1 with the highest score comprehends the top functions cancer, cellular movement and gastrointestinal disease. Network 2 contains the top functions endocrine system development and function, small molecule biochemistry and posttranslational modification.

The coefficient with the highest suppression (**0.25**) of gene expression was detected on the Homo sapiens connective tissue growth factor (*CTGF*) gene (NM_005328.1), whose product was first documented in 1991 [87]. The CTGF gene as well as the protein are well documented [88]; the search with

"CTGF "in PubMed (2012 July 24) found 295 hits since 1991. CTGF is located at cytogenetic band **6q23.1** by which a mitogen is encoded and secreted by vascular endothelial cells. The gene product is involved in chondrocyte proliferation and differentiation (GO: 0030154) [89; 90], in wound healing and in cell adhesion processes (GO:0007160) [91]. CTGF dysfunction is linked with a higher incidence of sclerosis and with a variety of fibrotic disorders. The association of the CTGF gene expression with a poor survival in hepatocellular carcinoma (HCC) patients is documented [92].

The CTGF downregulation may inhibit the growth of HCC cells [93], the growth and invasion of gastric cancer and its peritoneal dissemination [94], and the growth of papillary thyroid cancer cells [95]. This phenomenon should be taken in consideration in the development of therapeutic approaches in the patient-specific medicine. But inverse pharmacological effects, like the CTGF-mediated MMPs' downregulation in rheumatoid arthritis [96] and inhibition of cell motility and COX-2 expression in oral cancer cells [97], are observed. The role of CTGF in the follicle development and ovulation is documented [98].

We found a suppression of NM_000365.5, the homo sapiens triosephosphate isomerase (*TPII*) with the coefficient **0.35**. The UniProtKB knowledge-based documents the *TPII* gene encoding an enzyme [99], consisting of two identical proteins, which catalyze the isomerization of glyceraldehyde-3-phosphate (G3P) and dihydroxy-acetone phosphate (DHAP) in glycolysis and gluconeogenesis (http://www.uniprot.org/ uniprot/ B7Z5D8). *TPII* is mapped at **12p13.31** [100]. The gene coding the TPI1 offers a high amino acid sequence homology down to the *Bacillus stearothermophilus* enzyme (37%) but catalytically important residues are conserved [101].

TPII deregulation or single mutations cause enzyme deficiency resulting in dramatic consequences on the entire metabolisms [102], well documented also in the OMIM database (http://www.omim.org/ entry/190450). GO data "Biological process" indicate a pivotal role in the embryo development (GO: 0009790). The dysregulation of glycolysis correlates to manifold disease patterns like the increased Parkin expression demonstrated by proteomic analysis studies [103] and in the NextBio research database which documents genetically-caused diseases (TPI1 diseases).

Also a suppression of homo sapiens G protein coupled receptor (*GPR1*) with the coefficient **0.44** was detected (NM_005279.3). The *GPR1* was isolated in 1994 by the O'Dowd group [104; 105]. It is mapped at **2q33.3** and encodes for a G protein-coupled receptor for the inflammation-associated leukocyte chemoattractant chemerin/RARRES2 [retinoic acid receptor responder (tazarotene induced) 2] considered as an adipokine in children [106], as well as for a putative membrane-bound G protein, associated in the activation of cAMP synthesis [107]. GPR1 protein's role as a coreceptor for HIV-1 is supported by the literature [108-110]. The GPR1 G protein-coupled receptor suggests an association with respiratory distress syndrome (RDS). An altered expression may play a critical role in the pathogenesis of RDS in preterm infants [111].

Several predicted or hypothetical genes are also suppressed, namely XR_038750.1 [Predicted: homo sapiens (LOC148430)] with the coefficient **0.46** in the smoke probe and in the filter probe with the coefficient **0.41** (Table 7). The NCBI database Gene describes the gene symbol *LOC148430* as a ribosomal protein S2 pseudogene mapped at **1q23.3a**.

Also reduction of NG_010039 [Predicted: homo sapiens similar to ribosomal protein S2, transcript variant 3 (LOC440589)] with the coefficient **0.47**. The NCBI database Gene describes the official gene symbol *RPS2P8* as a ribosomal protein S2 pseudogene 8 mapped at **1p32.3**.

Also reduced was the NM_002952.3 corresponding to the gene *RPS2* which encodes the RPS2, ribosomal protein S2. Here we detect a down-regulation with the coefficient **0.48**. The gene is mapped at **16p13.3**. Finally, we found a suppression of XR_019262.2 [Predicted: homo sapiens (LOC402112)] with the coefficient **0.48**. The NCBI database Gene describes the official gene symbol *LOC402112* as an uncharacterized heterogeneous nuclear ribonucleoprotein A1 pseudogene mapped at **2q31.1f**. Annotations of these 4 genes are not available.

TABLE 6: AFFECTED GENES – EXPRESSION RATIO 2H CONTROL & 2H AFTER EXPOSITION TO CIGARETTE FILTER EXTRACTS

TABLE 7: AFFECTED GENES – EXPRESSION RATIO 24H CONTROL & 24H AFTER EXPOSITION TO FILTER EXTRACTS.

Pathway and Network Analysis

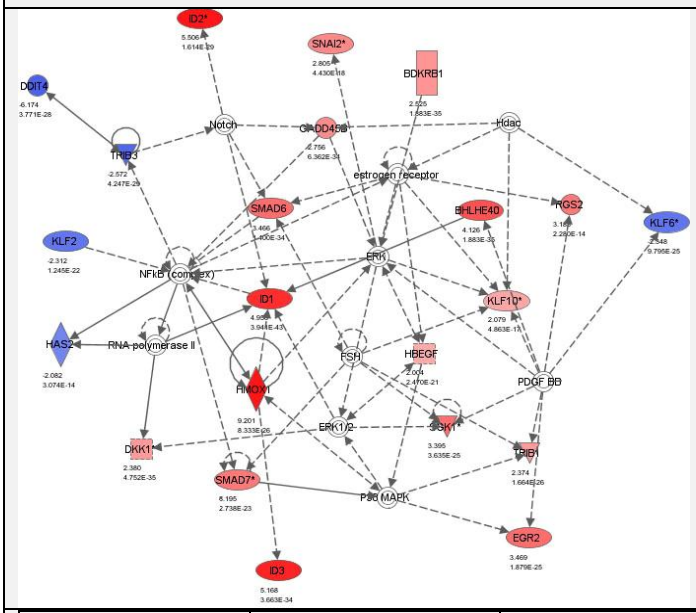

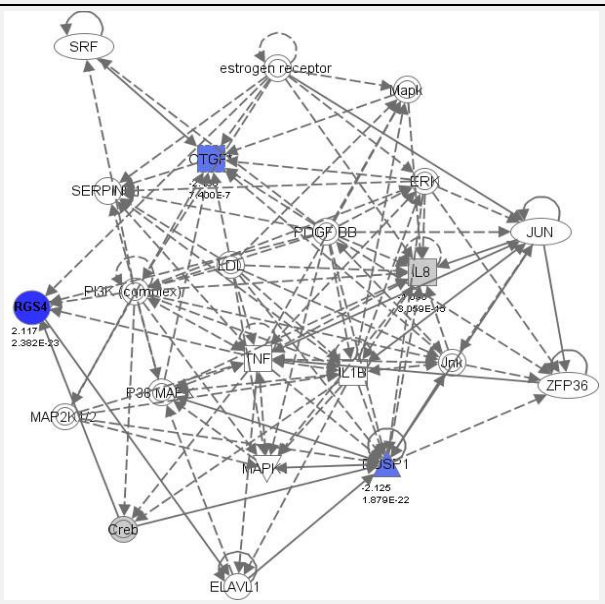

Gene Product (Gene)	RefSeq AC No.	Ratio filter 2 h/ control
HMOX1	NM_002133.2	**8.56**
ID2	NM_010496.3	**5.71**
ID3	NM_008321.2	**4.98**
ID1	NM_181353.1	**4.94**
RASL11B	NM_023940.2	**4.45**

Gene Product (Gene)	RefSeq AC No.	Ratio filter 24 h/ control
HAS2	NM_005328.1	**0.38**
Predicted ***LOC148430***	XR_018751.2	**0.41**
RGS4	NM_005613.5	**0.48**
GAS6	NM_00114395.1	**0.49**

Table 6 and Table 7 list the most affected genes with a rapid cellular response 2 h and 24 h after exposition to tobacco smoke components which are extracted from cigarette filters compared to untreated HEL cells as a control. It is evident that all coefficients reveal an increased gene expression induced as a rapid cellular stress response and suppressed expression as a late stress response (as listed in Table 2 and Table 3) and additionally compared to pyrolyzed tobacco smoke. Furthermore the following genes feature consistently a late suppression.

We detected a suppressed expression after 24 hours (**0.38**) in NM_005328.1. The NM_005328.1 describes the homo sapiens hyaluronan synthase 2 (*HAS2*) gene, which is mapped at **8q24.13a**.

It is responsible for the synthesis of hyaluronan or hyaluronic acid (HA), a polysaccharide with a high molecular weight which is a key constituent of the extracellular matrix. The search (2012 July 24) in the NCBI database "PubMed" finds 356 hits and confirms the physiological and biochemical significance of the *HAS2* gene, which was first identified by Watanabe and Yamaguchi in 1996 [112]. The Gene Ontology (GO: 0005887) shows a localization in the plasma membrane. The GO "molecular function" (GO: 0050501) of the protein indicates a hyaluronan synthase activity and the GO "biological process" (GO: 0030213) document the role of the chemical reactions and pathways resulting in the formation of hyaluronan [113]. The expression of HA is strongly controlled during wound healing and tissue repair processes [114].

Changes in the HA's serum concentration may result in inflammatory and degenerative arthropathies such as rheumatoid arthritis [115].

We also measured a repression (**0.48**) of the NCBI NM_005613.5 which is defined as the homo sapiens regulator of G protein signalling 4 (RGS4), transcript variant 2 mRNA, mapped at **1q23.3**. It encodes a G protein variant, member of the GTPase activating protein family, first characterized in 1996 [116]. The Gene Ontology (GO:0005624) shows the cytoplasm as localization connected with the inner membrane. The GO "molecular function" (GO: 0005096) indicates that the RGS4 protein inhibits signal transduction, the process by which extracellular signals induce intracellular responses [117]. The GO "biological process" (GO: 0000188) documents the role as the terminator of the activity of the active enzyme MAP kinase. The *RGS4* gene is expressed in brain and heart [118]. Deregulation and genetic variations in *RGS4* are also associated with susceptibility to multifactorial psychotic disorders [119; 120].

The search with NM_00114395.1 in the NCBI database "Gene" identifies the homo sapiens growth arrest-specific 6 gene (*GAS6*) gene (http://www.ncbi.nlm.nih.gov/gene?term=GAS6). The annotations of the *GAS6* gene were updated 2012 July 20. *GAS6* maps to **13q34d** and encodes the gamma-carboxyglutamic acid (Gla)-containing protein, thought to be involved in the stimulation of cell proliferation, and may play a role in thrombosis as first published in 1995 [121-123].

The Gene Ontology (GO: 0005615) shows the extracellular space as localization. The GO "molecular function" (GO: 0048018) indicates that the GAS6 protein features receptor agonist activity. The GO "biological process" (GO: 0043277) documents its role in an apoptotic cell removal and in blood clotting (GO: 0007596). We speculate that cellular stress derived from chemical noxes of cigarette smoke can suppress physiological processes, shown as a late effect (**0.49**) 24 hours after exposure.

The IPA analysis of the 2 h probe detected the following top networks. Network 1, shown in Table 6, comprehends the associated network functions cellular development cell death and survival.

The 24 h probe detected only one top network (shown in Table 7). The networks are the bases for recognition of the graphical pathway analyses.

CONCLUSION: The purpose of this study was the identification of differentially expressed genes after exposure to cigarette smoke components using a system able to gain explanations not restricted to a limited number of molecular- or cell-related events. With this microarray approach the analysis of the whole genome was necessary to study expression processes from the clinical point of view.

A series of modulated cellular processes responsible for the potential origin of illness and progression could be identified. Moreover, the inductive effects of tobacco smoke (TS) on xenobiotic metabolizing enzymes may help to explain reduced efficacy of chemotherapy, and to suggest targets for chemopreventive agents in smokers [67; 124]. Oxidative stress causes injury to lung cells and afterwards can lead to various diseases not restricted to the lung as comprehensively documented.

It is also uncontroversial that the surface-forming epithelial cells are most affected by teratogenic noxae and poisonous chemicals originating from polluted environment [125]. Whereas the gene toxic effects of tobacco smoke components and the consequences are intensively discussed, the cigarette's smoke influence on the gene expression in embryonic lung cells is far less intensively investigated. The search of January 11 2012 using the key words "tobacco smoke", "lung cells", and "gene expression" in the NCBI database PubMed resulted in only two publications illustrating smoke-induced gene families encoding metabolizing enzymes [126; 127] thus emphasizing the necessity for further investigations also in passive smokers [128-130].

Analytical differential gene expression studies of the impact of tobacco smoke on the cellular stress response should contribute to a better understanding of the processes leading to early children's indispositions and health consequences in the adulthood. We therefore analyzed the genes after short term (2h) and long term (24h) exposure of our extracts.

The data listed in the Table 3, Table 6 and Table 7 accentuate the cigarette filter potential to retain and refine tobacco smoke components. Unfortunately, as it is difficult or even impossible to dissuade the manhood from tobacco consumption, one possibility to decrease the smoking-related health hazards is to improve the effectiveness of cigarette filters. The functionalization of the filter's matrix surface with mixtures of chemical additives that solely improve the taste and the nicotine's uptake rate into the brain cannot be the right way in the cigarette filter research [131-134]. Consequently, the cigarette smoking is said to be the most important chief cause of preventable morbidity and premature mortality worldwide.

Our results reveal that more efficient filters would be able to remove dangerous substances from the smokers. Therefore we also performed alkaline and acidic filter extracts to learn better optimizing the ab- and adsorption properties of the filters. .

Generally, changes in the gene expression were also induced by the passive smoking. Children of smoker families hold the "wolf by the ears" by living in the same household [135; 136]. The exposure of young children to cigarette smoke enhances the risk for cardiovascular diseases, myocardial infarction, and strokes, as documented in a survey in south-west Germany conducted by the Koenig group in 2009 [137].

We emphasize that the purpose of this study was not to detail the smallest differential gene expression variants but to point out to what extend pyrolyzed smoke substances may influence gene expression using human HEL cells as an example. Our findings should contribute to additional insights into the exceedingly complex degenerative tobacco smoke scenario and open the discussion providing additional sound arguments against cigarette tobacco smoking especially without using effective filters.

Essence and purpose of the manuscript are not to appeal for a crusade against the tobacco consumption, a battle we are certain to lose due to the fact that it attends the whole human cultural history. Instead the data interpretation intensify the discussion and to gain a judicious behaviour. Particularly, with regard to the disastrous consequences for the development of unborn children, small children during adolescence, and finally for adults with a disease which could be anticipated years in advance. Lastly, an advice at first hand: 'Now that I'm gone, I tell you: don't smoke, whatever you do, just don't smoke' Yul Brynner (1920-1985) [138].

ACKNOWLEDGMENTS: The authors would like to thank Esther Densing, Aline Dupont and Alexander Schlich for the technical support.

Conflict of Interest: The authors declare herewith no financial or commercial conflict of interest.

REFERENCES:

1. WHO Report on the Global Tobacco Epidemic, 2011 - Warning about the dangers of tobacco-. In: Anonymous. Geneva: World Health Organization, 2011; 1-150.
2. Mills AL, Messer K, Gilpin EA, *et al*. The effect of smoke-free homes on adult smoking behavior: A review. Nicotine Tob Res 2009; 11 (10): 1131-1141.
3. Boulesteix AL, Slawski M. Stability and aggregation of ranked gene lists. Brief Bioinform 2009; 10 (5): 556-568.
4. Agutter PS. Cell mechanics and stress: from molecular details to the 'universal cell reaction' and hormesis. 2007; 29 (4): 324-333.
5. Tiligada E. Chemotherapy: induction of stress responses. Endocr Relat Cancer 2006; 13 Suppl 1: S115-S124.
6. Saiki T. Liquid Extraction with the Aid of Soxhlet's Apparatus . J Biol Chem 1909; 7 (1): 21-22.
7. Eberwine J, Spencer C, Miyashiro K, *et al*. Complementary DNA synthesis in situ: methods and applications. Methods Enzymol 1992; 216: 80-100.
8. Bolstad B. Probe Level Quantile Normalization of High Density Oligonucleotide Array Data. 2001; 1-8.
9. Benjamini Y, Hochberg Y. Controlling the False Discovery Rate - A Practical and Powerful Approach to Multiple Testing. 1995; 57 (1): 289-300.
10. Eisen MB, Spellman PT, Brown PO, *et al*. Cluster analysis and display of genome-wide expression patterns. Proc Natl Acad Sci U S A 1998; 95 (25): 14863-14868.
11. Ingenuity Pathways Analysis ("IPA"), Ingenuity® Systems, www.ingenuity.com . 2013.
12. Fan JB, Gunderson KL, Bibikova M, *et al*. Illumina universal bead arrays. Methods Enzymol 2006; 410: 57-73.
13. Dunning MJ, Barbosa-Morais NL, Lynch AG, *et al*. Statistical issues in the analysis of Illumina data. BMC Bioinformatics 2008; 9: 85.
14. Bodnar JA, Morgan WT, Murphy PA, *et al*. Mainstream smoke chemistry analysis of samples from the 2009 US cigarette market. Regul Toxicol Pharmacol 2012; 64 (1): 35-42.
15. Wilson CL, Bodnar JA, Brown BG, *et al*. Assessment of dioxin and dioxin-like compounds in mainstream smoke from selected US cigarette brands and reference cigarettes. Food Chem Toxicol 2008; 46 (5): 1721-1733.
16. Mariner D, Shepperd J. Special supplement introduction: Estimating cigarette smoke exposure by filter analysis. Regul Toxicol Pharmacol 2011; 61 (3 Suppl): S1-S2.
17. Shepperd CJ, Eldridge AC, Mariner DC, *et al*. A study to estimate and correlate cigarette smoke exposure in smokers in Germany as determined by filter analysis and

biomarkers of exposure. Regul Toxicol Pharmacol 2009; 55 (1): 97-109.
18. Harris B. The intractable cigarette 'filter problem'. 2011; 20: I10-I16.
19. Healton CG, Cummings KM, O'Connor RJ, *et al*. Butt really? The environmental impact of cigarettes. Tob Control 2011; 20 Suppl 1: i1.
20. Pickett G, Seagrave J, Boggs S, *et al*. Effects of 10 cigarette smoke condensates on primary human airway epithelial cells by comparative gene and cytokine expression studies. Toxicol Sci 2010; 114 (1): 79-89.
21. Gerhard DS, Wagner L, Feingold EA, *et al*. The status, quality, and expansion of the NIH full-length cDNA project: the Mammalian Gene Collection (MGC). Genome Res 2004; 14 (10B): 2121-2127.
22. Fu H, Subramanian RR, Masters SC. 14-3-3 proteins: structure, function, and regulation. Annu Rev Pharmacol Toxicol 2000; 40: 617-647.
23. Vadysirisack DD, Ellisen LW. mTOR activity under hypoxia. Methods Mol Biol 2012; 821: 45-58.
24. Hulmi JJ, Silvennoinen M, Lehti M, *et al*. Altered REDD1, myostatin, and Akt/mTOR/FoxO/MAPK signaling in streptozotocin-induced diabetic muscle atrophy. Am J Physiol Endocrinol Metab 2012; 302 (3): E307-E315.
25. Lupke M, Frahm J, Lantow M, *et al*. Gene expression analysis of ELF-MF exposed human monocytes indicating the involvement of the alternative activation pathway. Biochim Biophys Acta 2006; 1763 (4): 402-412.
26. Hara E, Yamaguchi T, Nojima H, *et al*. Id-related genes encoding helix-loop-helix proteins are required for G1 progression and are repressed in senescent human fibroblasts. J Biol Chem 1994; 269 (3): 2139-2145.
27. Mathew S, Chen W, Murty VV, *et al*. Chromosomal assignment of human ID1 and ID2 genes. 1995; 30 (2): 385-387.
28. Kim HJ, Kim JY, Park YY, *et al*. Synergistic activation of the human orphan nuclear receptor SHP gene promoter by basic helix-loop-helix protein E2A and orphan nuclear receptor SF-1. Nucleic Acids Res 2003; 31 (23): 6860-6872.
29. Lai C, Loo G. Cellular iron depletion weakens induction of heme oxygenase-1 by cadmium. Int J Biochem Cell Biol 2011; 43 (1): 88-97.
30. Pulkkinen KH, Yla-Herttuala S, Levonen AL. Heme oxygenase 1 is induced by miR-155 via reduced BACH1 translation in endothelial cells. Free Radic Biol Med 2011; 51 (11): 2124-2131.
31. Warnatz HJ, Schmidt D, Manke T, *et al*. The BTB and CNC homology 1 (BACH1) target genes are involved in the oxidative stress response and in control of the cell cycle. J Biol Chem 2011; 286 (26): 23521-23532.
32. Fratta PA, Albiero A, Stranieri C, *et al*. Serum oxidative stress-induced repression of Nrf2 and GSH depletion: a mechanism potentially involved in endothelial dysfunction of young smokers. PLoS One 2012; 7 (1): e30291.
33. Evstatiev R, Gasche C. Iron sensing and signalling. 2012; 61 (6): 933-952.
34. Immenschuh S, Baumgart-Vogt E, Mueller S. Heme oxygenase-1 and iron in liver inflammation: a complex alliance. Curr Drug Targets 2010; 11 (12): 1541-1550.
35. Schroder K, Zhang M, Benkhoff S, *et al*. Nox4 is a protective reactive oxygen species generating vascular NADPH oxidase. Circ Res 2012; 110 (9): 1217-1225.
36. Hefferan TE, Reinholz GG, Rickard DJ, *et al*. Overexpression of a nuclear protein, TIEG, mimics transforming growth factor-beta action in human osteoblast cells. J Biol Chem 2000; 275 (27): 20255-20259.
37. Blok LJ, Grossmann ME, Perry JE, *et al*. Characterization of an early growth response gene, which encodes a zinc finger transcription factor, potentially involved in cell cycle regulation. Mol Endocrinol 1995; 9 (11): 1610-1620.
38. Chrisman HR, Tindall DJ. Identification and characterization of a consensus DNA binding element for the zinc finger transcription factor TIEG/EGRalpha. DNA Cell Biol 2003; 22 (3): 187-199.
39. Reinholz MM, An MW, Johnsen SA, *et al*. Differential gene expression of TGF beta inducible early gene (TIEG), Smad7, Smad2 and Bard1 in normal and malignant breast tissue. Breast Cancer Res Treat 2004; 86 (1): 75-88.
40. Song KD, Kim DJ, Lee JE, *et al*. KLF10, transforming growth factor-?-inducible early gene 1, acts as a tumor suppressor. 2012; 419 (2): 388-394.
41. Ivanov SV, Ivanova AV, Salnikow K, *et al*. Two novel VHL targets, TGFBI (BIGH3) and its transactivator KLF10, are up-regulated in renal clear cell carcinoma and other tumors. 2008; 370 (4): 536-540.
42. Shiga K, Noto Y, Mizuta I, *et al*. A novel EGR2 mutation within a family with a mild demyelinating form of Charcot-Marie-Tooth disease. J Peripher Nerv Syst 2012; 17 (2): 206-209.
43. Baets J, Deconinck T, De VE, *et al*. Genetic spectrum of hereditary neuropathies with onset in the first year of life. 2011; 134 (Pt 9): 2664-2676.
44. Bellone E, Di ME, Soriani S, *et al*. A novel mutation (D305V) in the early growth response 2 gene is associated with severe Charcot-Marie-Tooth type 1 disease. Hum Mutat 1999; 14 (4): 353-354.
45. Funalot B, Topilko P, Arroyo MA, *et al*. Homozygous deletion of an EGR2 enhancer in congenital amyelinating neuropathy. Ann Neurol 2012; 71 (5): 719-723.
46. Charnay P, Coulpier F, Decker L, *et al*. [Krox20 inactivation in the PNS leads to CNS/PNS boundary transgression by central glia]. Bull Acad Natl Med 2010; 194 (4-5): 743-744.
47. Selvakumaran M, Lin HK, Sjin RT, *et al*. The novel primary response gene MyD118 and the proto-oncogenes myb, myc, and bcl-2 modulate transforming growth factor beta 1-induced apoptosis of myeloid leukemia cells. Mol Cell Biol 1994; 14 (4): 2352-2360.
48. Liebermann DA, Hoffman B. MyD genes in negative growth control. 1998; 17 (25): 3319-3329.
49. Michaelis KA, Knox AJ, Xu M, *et al*. Identification of growth arrest and DNA-damage-inducible gene beta (GADD45beta) as a novel tumor suppressor in pituitary gonadotrope tumors. 2011; 152 (10): 3603-3613.
50. Selvakumaran M, Lin HK, Miyashita T, *et al*. Immediate early up-regulation of bax expression by p53 but not TGF beta 1: a paradigm for distinct apoptotic pathways. Oncogene 1994; 9 (6): 1791-1798.
51. Guillouf C, Rosselli F, Krishnaraju K, *et al*. p53 involvement in control of G2 exit of the cell cycle: role in DNA damage-induced apoptosis. 1995; 10 (11): 2263-2270.
52. Liebermann DA, Hoffman B. Gadd45 in the response of hematopoietic cells to genotoxic stress. Blood Cells Mol Dis 2007; 39 (3): 329-335.
53. Hoffman B, Liebermann DA. Gadd45 modulation of intrinsic and extrinsic stress responses in myeloid cells. J Cell Physiol 2009; 218 (1): 26-31.
54. Gurda GT, Wang JY, Guo L, *et al*. Profiling CCK-mediated pancreatic growth: the dynamic genetic program and the role of STATs as potential regulators. Physiol Genomics 2012; 44 (1): 14-24.

55. Kaufmann LT, Niehrs C. Gadd45a and Gadd45g regulate neural development and exit from pluripotency in Xenopus. Mech Dev 2011; 128 (7-10): 401-411.
56. Kaufmann LT, Gierl MS, Niehrs C. Gadd45a, Gadd45b and Gadd45g expression during mouse embryonic development. Gene Expr Patterns 2011; 11 (8): 465-470.
57. Speisky D, Duces A, Bieche I, *et al*. Molecular profiling of pancreatic neuroendocrine tumors in sporadic and Von Hippel-Lindau patients. Clin Cancer Res 2012; 18 (10): 2838-2849.
58. Iida M, Anna CH, Gaskin ND, *et al*. The putative tumor suppressor Tsc-22 is downregulated early in chemically induced hepatocarcinogenesis and may be a suppressor of Gadd45b. Toxicol Sci 2007; 99 (1): 43-50.
59. Ying J, Srivastava G, Hsieh WS, *et al*. The stress-responsive gene GADD45G is a functional tumor suppressor, with its response to environmental stresses frequently disrupted epigenetically in multiple tumors. Clin Cancer Res 2005; 11 (18): 6442-6449.
60. Vairapandi M, Balliet AG, Fornace AJ, Jr., *et al*. The differentiation primary response gene MyD118, related to GADD45, encodes for a nuclear protein which interacts with PCNA and p21WAF1/CIP1. 1996; 12 (12): 2579-2594.
61. Vairapandi M, Azam N, Balliet AG, *et al*. Characterization of MyD118, Gadd45, and proliferating cell nuclear antigen (PCNA) interacting domains. PCNA impedes MyD118 AND Gadd45-mediated negative growth control. J Biol Chem 2000; 275 (22): 16810-16819.
62. Thompson CA, Burcham PC. Genome-wide transcriptional responses to acrolein. Chem Res Toxicol 2008; 21 (12): 2245-2256.
63. McLellan RA, Oscarson M, Hidestrand M, *et al*. Characterization and functional analysis of two common human cytochrome P450 1B1 variants. Arch Biochem Biophys 2000; 378 (1): 175-181.
64. Reddy VV, Hanjani P, Rajan R. Synthesis of catechol estrogens by human uterus and leiomyoma. Steroids 1981; 37 (2): 195-203.
65. Theron CN, Russell VA, Taljaard JJ. Evidence that estradiol-2/4-hydroxylase activities in rat hypothalamus and hippocampus differ qualitatively and involve multiple forms of P-450: ontogenetic and inhibition studies. J Steroid Biochem 1985; 23 (6A): 919-927.
66. Ikegwuonu FI, Christou M, Jefcoate CR. Regulation of cytochrome P4501B1 (CYP1B1) in mouse embryo fibroblast (C3H10T1/2) cells by protein kinase C (PKC). Biochem Pharmacol 1999; 57 (6): 619-630.
67. Gumus ZH, Du B, Kacker A, *et al*. Effects of tobacco smoke on gene expression and cellular pathways in a cellular model of oral leukoplakia. Cancer Prev Res (Phila) 2008; 1 (2): 100-111.
68. Ito T, Nagai H, Lin TM, *et al*. Organic Chemicals Adsorbed onto Diesel Exhaust Particles Directly Alter the Differentiation of Fetal Thymocytes Through Arylhydrocarbon Receptor but Not Oxidative Stress Responses. J Immunotoxicol 2006; 3 (1): 21-30.
69. Diani-Moore S, Ram P, Li X, *et al*. Identification of the aryl hydrocarbon receptor target gene TiPARP as a mediator of suppression of hepatic gluconeogenesis by 2,3,7,8-tetrachlorodibenzo-p-dioxin and of nicotinamide as a corrective agent for this effect. J Biol Chem 2010; 285 (50): 38801-38810.
70. Aung HH, Lame MW, Gohil K, *et al*. Comparative gene responses to collected ambient particles in vitro: endothelial responses. Physiol Genomics 2011; 43 (15): 917-929.
71. Katoh M, Katoh M. Identification and characterization of human TIPARP gene within the CCNL amplicon at human chromosome 3q25.31. Int J Oncol 2003; 23 (2): 541-547.
72. Boutros PC, Yao CQ, Watson JD, *et al*. Hepatic transcriptomic responses to TCDD in dioxin-sensitive and dioxin-resistant rats during the onset of toxicity. Toxicol Appl Pharmacol 2011; 251 (2): 119-129.
73. Ma Q, Baldwin KT, Renzelli AJ, *et al*. TCDD-inducible poly(ADP-ribose) polymerase: a novel response to 2,3,7,8-tetrachlorodibenzo-p-dioxin. Biochem Biophys Res Commun 2001; 289 (2): 499-506.
74. Teramoto M, Nakamasu K, Noshiro M, *et al*. Gene structure and chromosomal location of a human bHLH transcriptional factor DEC1 x Stra13 x SHARP-2/BHLHB2. J Biochem 2001; 129 (3): 391-396.
75. Shen M, Kawamoto T, Yan W, *et al*. Molecular characterization of the novel basic helix-loop-helix protein DEC1 expressed in differentiated human embryo chondrocytes. Biochem Biophys Res Commun 1997; 236 (2): 294-298.
76. Honma S, Kawamoto T, Takagi Y, *et al*. Dec1 and Dec2 are regulators of the mammalian molecular clock. 2002; 419 (6909): 841-844.
77. Nakashima A, Kawamoto T, Honda KK, *et al*. DEC1 modulates the circadian phase of clock gene expression. Mol Cell Biol 2008; 28 (12): 4080-4092.
78. Li Y, Xie M, Song X, *et al*. DEC1 negatively regulates the expression of DEC2 through binding to the E-box in the proximal promoter. J Biol Chem 2003; 278 (19): 16899-16907.
79. Cheli Y, Giuliano S, Fenouille N, *et al*. Hypoxia and MITF control metastatic behaviour in mouse and human melanoma cells. 2012; 31 (19): 2461-2470.
80. Holtkamp N, Ziegenhagen N, Malzer E, *et al*. Characterization of the amplicon on chromosomal segment 4q12 in glioblastoma multiforme. Neuro Oncol 2007; 9 (3): 291-297.
81. Kresse SH, Meza-Zepeda LA, Machado I, *et al*. Preclinical xenograft models of human sarcoma show nonrandom loss of aberrations. 2012; 118 (2): 558-570.
82. Bechtel S, Rosenfelder H, Duda A, *et al*. The full-ORF clone resource of the German cDNA Consortium. BMC Genomics 2007; 8: 399.
83. Rampazzo A, Pivotto F, Occhi G, *et al*. Characterization of C14orf4, a novel intronless human gene containing a polyglutamine repeat, mapped to the ARVD1 critical region. Biochem Biophys Res Commun 2000; 278 (3): 766-774.
84. Rampazzo A, Nava A, Danieli GA, *et al*. The gene for arrhythmogenic right ventricular cardiomyopathy maps to chromosome 14q23-q24. Hum Mol Genet 1994; 3 (6): 959-962.
85. Beausoleil SA, Jedrychowski M, Schwartz D, *et al*. Large-scale characterization of HeLa cell nuclear phosphoproteins. Proc Natl Acad Sci U S A 2004; 101 (33): 12130-12135.
86. Heger S, Mastronardi C, Dissen GA, *et al*. Enhanced at puberty 1 (EAP1) is a new transcriptional regulator of the female neuroendocrine reproductive axis. J Clin Invest 2007; 117 (8): 2145-2154.
87. Bradham DM, Igarashi A, Potter RL, *et al*. Connective tissue growth factor: a cysteine-rich mitogen secreted by human vascular endothelial cells is related to the SRC-induced immediate early gene product CEF-10. J Cell Biol 1991; 114 (6): 1285-1294.
88. Igarashi A, Bradham DM, Okochi H, *et al*. Connective tissue growth factor. J Dermatol 1992; 19 (11): 642-643.

89. Nakanishi T, Nishida T, Shimo T, *et al*. Effects of CTGF/Hcs24, a product of a hypertrophic chondrocyte-specific gene, on the proliferation and differentiation of chondrocytes in culture. 2000; 141 (1): 264-273.
90. Shimo T, Nakanishi T, Nishida T, *et al*. Connective tissue growth factor induces the proliferation, migration, and tube formation of vascular endothelial cells in vitro, and angiogenesis in vivo. J Biochem 1999; 126 (1): 137-145.
91. Abraham DJ, Shiwen X, Black CM, *et al*. Tumor necrosis factor alpha suppresses the induction of connective tissue growth factor by transforming growth factor-beta in normal and scleroderma fibroblasts. J Biol Chem 2000; 275 (20): 15220-15225.
92. Xiang ZL, Zeng ZC, Fan J, *et al*. Expression of connective tissue growth factor and interleukin-11 in intratumoral tissue is associated with poor survival after curative resection of hepatocellular carcinoma. 2012; 39 (5): 6001-6006.
93. Jia XQ, Cheng HQ, Li H, *et al*. Inhibition of connective tissue growth factor overexpression decreases growth of hepatocellular carcinoma cells in vitro and in vivo. 2011; 124 (22): 3794-3799.
94. Jiang CG, Lv L, Liu FR, *et al*. Downregulation of connective tissue growth factor inhibits the growth and invasion of gastric cancer cells and attenuates peritoneal dissemination. 2011; 10.
95. Cui L, Zhang Q, Mao ZF, *et al*. CTGF is overexpressed in papillary thyroid carcinoma and promotes the growth of papillary thyroid cancer cells. 2011; 32 (4): 721-728.
96. Wang JG, Ruan J, Li CY, *et al*. Connective tissue growth factor, a regulator related with 10-hydroxy-2-decenoic acid down-regulate MMPs in rheumatoid arthritis. Rheumatol Int 2011.
97. Chuang JY, Yang WY, Lai CH, *et al*. CTGF inhibits cell motility and COX-2 expression in oral cancer cells. 2011; 11 (8): 948-954.
98. Nagashima T, Kim J, Li QL, *et al*. Connective Tissue Growth Factor Is Required for Normal Follicle Development and Ovulation. 2011; 25 (10): 1740-1759.
99. Brown JR, Daar IO, Krug JR, *et al*. Characterization of the functional gene and several processed pseudogenes in the human triosephosphate isomerase gene family. Mol Cell Biol 1985; 5 (7): 1694-1706.
100. Law ML, Kao FT. Regional Assignment of Human Genes Tpi1, Gapdh, Ldhb, Shmt, and Pepb on Chromosome-12. 1979; 24 (2): 102-114.
101. Alber T, Kawasaki G. Nucleotide sequence of the triose phosphate isomerase gene of Saccharomyces cerevisiae. J Mol Appl Genet 1982; 1 (5): 419-434.
102. Watanabe M, Zingg BC, Mohrenweiser HW. Molecular analysis of a series of alleles in humans with reduced activity at the triosephosphate isomerase locus. Am J Hum Genet 1996; 58 (2): 308-316.
103. Davison EJ, Pennington K, Hung CC, *et al*. Proteomic analysis of increased Parkin expression and its interactants provides evidence for a role in modulation of mitochondrial function. Proteomics 2009; 9 (18): 4284-4297.
104. Marchese A, Docherty JM, Nguyen T, *et al*. Cloning of human genes encoding novel G protein-coupled receptors. 1994; 23 (3): 609-618.
105. Heiber M, Docherty JM, Shah G, *et al*. Isolation of three novel human genes encoding G protein-coupled receptors. DNA Cell Biol 1995; 14 (1): 25-35.
106. Landgraf K, Friebe D, Ullrich T, *et al*. Chemerin as a Mediator between Obesity and Vascular Inflammation in Children. 2012; 97 (4): E556-E564.
107. Xue Y, Batlle M, Hirsch JP. GPR1 encodes a putative G protein-coupled receptor that associates with the Gpa2p Galpha subunit and functions in a Ras-independent pathway. EMBO J 1998; 17 (7): 1996-2007.
108. Shimizu N, Tanaka A, Jinno-Oue A, *et al*. Short Communication: Identification of the Conformational Requirement for the Specificities of Coreceptors for Human and Simian Immunodeficiency Viruses. 2010; 26 (3): 321-328.
109. Jinno-Oue A, Shimizu N, Soda Y, *et al*. The synthetic peptide derived from the NH2-terminal extracellular region of an orphan G protein-coupled receptor, GPR1, preferentially inhibits infection of X4 HIV-1. 2005; 280 (35): 30924-30934.
110. Singh A, Besson G, Mobasher A, *et al*. Patterns of chemokine receptor fusion cofactor utilization by human immunodeficiency virus type 1 variants from the lungs and blood. 1999; 73 (8): 6680-6690.
111. Pulkkinen V, Haataja R, Hannelius U, *et al*. G protein-coupled receptor for asthma susceptibility associates with respiratory distress syndrome. 2006; 38 (5): 357-366.
112. Watanabe K, Yamaguchi Y. Molecular identification of a putative human hyaluronan synthase. 1996; 271 (38): 22945-22948.
113. Li LL, Asteriou T, Bernert B, *et al*. Growth factor regulation of hyaluronan synthesis and degradation in human dermal fibroblasts: importance of hyaluronan for the mitogenic response of PDGF-BB. 2007; 404: 327-336.
114. Vigetti D, Genasetti A, Karousou E, *et al*. Proinflammatory Cytokines Induce Hyaluronan Synthesis and Monocyte Adhesion in Human Endothelial Cells through Hyaluronan Synthase 2 (HAS2) and the Nuclear Factor-kappa B (NF-kappa B) Pathway. 2010; 285 (32): 24639-24645.
115. Maroski J, Vorderwulbecke BJ, Fiedorowicz K, *et al*. Shear stress increases endothelial hyaluronan synthase 2 and hyaluronan synthesis especially in regard to an atheroprotective flow profile. 2011; 96 (9): 977-986.
116. Druey KM, Blumer KJ, Kang VH, *et al*. Inhibition of G-protein-mediated MAP kinase activation by a new mammalian gene family. 1996; 379 (6567): 742-746.
117. Popov SG, Krishna UM, Falck JR, *et al*. Ca2+/Calmodulin reverses phosphatidylinositol 3,4, 5-trisphosphate-dependent inhibition of regulators of G protein-signaling GTPase-activating protein activity. J Biol Chem 2000; 275 (25): 18962-18968.
118. Ding L, Mychaleckyj JC, Hegde AN. Full length cloning and expression analysis of splice variants of regulator of G-protein signaling RGS4 in human and murine brain. 2007; 401 (1-2): 46-60.
119. Chowdari KV, Mirnics K, Semwal P, *et al*. Association and linkage analyses of RGS4 polymorphisms in schizophrenia. 2002; 11 (12): 1373-1380.
120. Morris DW, Rodgers A, Mcghee KA, *et al*. Confirming RGS4 as a susceptibility gene for schizophrenia. 2004; 125B (1): 50-53.
121. Godowski PJ, Mark MR, Chen JA, *et al*. Reevaluation of the Roles of Protein-S and Gas6 As Ligands for the Receptor Tyrosine Kinase Rse/Tyro-3. 1995; 82 (3): 355-358.
122. Stitt TN, Conn G, Gore M, *et al*. The Anticoagulation Factor Protein-S and Its Relative, Gas6, Are Ligands for the Tyro 3/Axl Family of Receptor Tyrosine Kinases. 1995; 80 (4): 661-670.
123. Saccone S, Marcandalli P, Gostissa M, *et al*. Assignment of the Human Gas6 Gene to Chromosome 13Q34 by Fluorescence In-Situ Hybridization. 1995; 30 (1): 129-131.

124. Boyle JO, Gumus ZH, Kacker A, *et al*. Effects of cigarette smoke on the human oral mucosal transcriptome. Cancer Prev Res (Phila) 2010; 3 (3): 266-278.
125. O'Brien PJ, Hales BF, Josephy PD, *et al*. Chemical carcinogenesis, mutagenesis, and teratogenesis. Can J Physiol Pharmacol 1996; 74 (5): 565-571.
126. Villard PH, Seree EM, Re JL, *et al*. Effects of tobacco smoke on the gene expression of the Cyp1a, Cyp2b, Cyp2e, and Cyp3a subfamilies in mouse liver and lung: relation to single strand breaks of DNA. Toxicol Appl Pharmacol 1998; 148 (2): 195-204.
127. Thum T, Erpenbeck VJ, Moeller J, *et al*. Expression of xenobiotic metabolizing enzymes in different lung compartments of smokers and nonsmokers. Environ Health Perspect 2006; 114 (11): 1655-1661.
128. Zhang J, Liu Y, Shi J, *et al*. Side-Stream Cigarette Smoke Induces Dose-Response in Systemic Inflammatory Cytokine Production and Oxidative Stress. 2002; 227: 823-829.
129. Fiskin K, Ozkan A, Ayhan AG. Investigation of protective effects of selenium and vitamin E against DNA oxidation, membrane damage and alteration of COMT metabolism in smoke-exposed male mice (Mus musculus, Balb/c). Acta Biol Hung 2006; 57 (4): 403-413.
130. Scherer G, Conze C, Tricker AR, *et al*. Uptake of tobacco smoke constituents on exposure to environmental tobacco smoke (ETS). Clin Investig 1992; 70 (3-4): 352-367.
131. Kurien BT, Scofield RH. Bubbling hookah smoke through heat-solubilized curcumin/turmeric and incorporation of the curry spice as an additive or filter in cigarettes to minimize tobacco smoke-related toxicants. Med Hypotheses 2009; 73 (3): 462-463.
132. McAdam KG, Gregg EO, Liu C, *et al*. The use of a novel tobacco-substitute sheet and smoke dilution to reduce toxicant yields in cigarette smoke. Food Chem Toxicol 2011; 49 (8): 1684-1696.
133. Gordon SM, Brinkman MC, Meng RQ, *et al*. Effect of cigarette menthol content on mainstream smoke emissions. Chem Res Toxicol 2011; 24 (10): 1744-1753.
134. Pauly JL, Lee HJ, Hurley EL, *et al*. Glass fiber contamination of cigarette filters: an additional health risk to the smoker? Cancer Epidemiol Biomarkers Prev 1998; 7 (11): 967-979.
135. Tyc VL, Lensing S, Vukadinovich CM, *et al*. Can parents of children with cancer accurately report their child's passive smoking exposure? Nicotine Tob Res 2009; 11 (11): 1289-1295.
136. Piippo-Savolainen E, Korppi M. Long-term outcomes of early childhood wheezing. Curr Opin Allergy Clin Immunol 2009; 9 (3): 190-196.
137. Nagel G, Arnold FJ, Wilhelm M, *et al*. Environmental tobacco smoke and cardiometabolic risk in young children: results from a survey in south-west Germany. Eur Heart J 2009; 30 (15): 1885-1893.
138. Brynner Y. Now that I'm gone, I tell you: Don't smoke, whatever you do, just don't smoke. 'See Your Dentist - It Can Save Your Life,' Zila Pharmaceuticals, Inc, Promoting Oral, Head and Neck Cancer Awareness Week, 2006; (April 17-22).

How to cite this article:
Braun K, Müller G, Schick M, Bewerunge-Hudler M, Heil O, Wiessler M, Pipkorn R, Semmler W and Waldeck W: Expressions profiling project of Human embryonic lung cells exposed to Pyrolyzed Cigarette smoke. *Int J Pharm Sci Res* 2013; 4(11): 4203-22. doi: 10.13040/IJPSR. 0975-8232.4(11).4203-22